ISTITUTO NAZIONALE DI FISICA NUCLEARE
Laboratori Nazionali di Frascati

LNF-85/39(P)
2 Agosto 1985

M. Greco:

COLLIDER PHYSICS AND THE STANDARD MODEL

Invited talk at the XVII Symposium on Multiparticle Dynamics, Kiryat-Anavim, Israel, 9-14 June 1985.

Servizio Documentazione
dei Laboratori Nazionali di Frascati
Cas. Postale 13 - Frascati (Roma)

COLLIDER PHYSICS AND THE STANDARD MODEL

M. Greco
INFN - Laboratori Nazionali di Frascati, P.O.Box 13 - 00044 Frascati (Italy)

ABSTRACT

Recent results at the $S\bar{p}pS$ collider are discussed in the framework of the electro-weak theory and perturbative QCD.

1. INTRODUCTION AND SUMMARY

The abundance of data on the $W^{\pm}$ and Z^0 weak bosons accumulated so far at the CERN $S\bar{p}pS$ collider has allowed detailed tests of the Standard Model confirming that fundamental interactions-electro-weak-strong- are described by gauge theories, in the presently explored range of energies and momentum transfers. Theoretically it has long been clear that the Standard Model is not complete. The origin of masses and the difficulties with the Higgs sector, the generation of flavours, the connection with gravity, are just some well known examples of the present limitations of the model and the reason for expecting departures from it in the Tev energy range. However none of last year's anomalies[1] in the collider's data that hinted at new physics has been confirmed so far with the increased statistics and improved analyses[2]. On the other hand the additional '84 data have provided more stringent tests of the Standard Model which is now in very good shape[3]. There are indeed no established data that cannot be explained by the Standard Model. Further precision tests of the theory and possible signals for new physics will emerge soon in the lepton and hadron colliders presently planned or under construction.

In the present talk I will present a comparison of the recent $S\bar{p}pS$ collider results[2] with the theoretical expectations. In Sect. 2 the present status of the electroweak theory and precision tests feasible in the next future will be reviewed. Vector boson production and related subjects an discussed in Sect. 3 in the framework of perturbative QCD. Then Sect. 4 reviews jet phenomena and related evidence for gluon effects, with a final short note on Higgs boson production.

2. PRECISION TESTS OF THE ELECTROWEAK THEORY[4]

To lowest order in the electroweak theory[5] the following basic relations are satisfied

$$s^2 \equiv \sin^2\theta_W = 1 - \frac{M_W^2}{M_Z^2} \qquad (1)$$

$$s^2 = \frac{\pi\alpha}{\sqrt{2}\,G_F}\,\frac{1}{M_W^2} \qquad (2)$$

The equality between Eqs. (1) and (2) is expected to be broken in simple extensions of the Standard Model, as, for example, for a Higgs sector with more than one doublet, for most compositeness schems, etc. On the other hand radiative corrections also modify the above relations. Thus the detailed evaluation of the radiative effects is an essential tool to test the electroweak theory.

For a comparison with experimental data on M_W and M_Z it is more convenient to use Eq. (1) as a definition of $\sin^2\theta_W$, assumed to hold exactly to any order of perturbation

theory, and to transfer thus all the effect of the corrections into a modification of Eq. (2)[6]. The latter becomes

$$s^2 = \frac{\pi\alpha(M)}{\sqrt{2}\, G_F} \quad \frac{1}{M_W^2}\,(1+\varepsilon), \tag{3}$$

and the various factors are discussed below. The e.m. coupling constant is taken at the scale $M=M_W \simeq M_Z$ and is obtained from the usual fine structure constant α as

$$\alpha^{-1}(M) = \alpha^{-1} - \frac{-2}{3\pi} \sum_f Q_f^2 \ln\left(\frac{M}{m_f}\right) + \frac{1}{6\pi} + \ldots$$

$$= 127.70 \pm 0.30 + \frac{8}{9\pi} \ln\left(\frac{m_t}{36\ \text{GeV}}\right), \tag{4}$$

where the summation is taken over all charged fermions with $m_f \leq M$. The light quark contribution is obtained from a dispersive analysis of $e^+e^- \rightarrow$ hadrons and the uncertainty ± 0.30 comes from e^+e^- data at low energies. The factor $\alpha(M)/\alpha = 1.073 \pm 0.003$ is indeed the dominant source of corrections to the W^+ and Z masses (see below).

Because of the absence of large logarithmic corrections to $G_F(M)/G_F(\mu)$, the scale depedence has been omitted in (4), and then the Fermi coupling constant is best defined from the precise determination of the muon lifetime[7]

$$\frac{1}{\tau_\mu} = \frac{G_F^2\, m_\mu^5}{192\,\pi^3} \left(1 - \frac{8m_e^2}{m_\mu^2}\right)\left(1 + \frac{3m_\mu^2}{5M_W^2}\right)\left[1 + \frac{\alpha}{2\pi}\left(\frac{25}{4} - \pi^2\right)\left(1 + \frac{2\alpha}{3\pi} \ln \frac{m_\mu}{m_e}\right)\right] \tag{5}$$

Finally the quantity ε in Eq. (3) contains the remaining - physically most interesting - corrections which would provide a precision test of the theory. It is customary to rewrite Eq. (3) in the form of a correction to the weak boson masses as follows

$$M_W = \cos\theta_W\, M_Z = \frac{\bar{M}}{s} \quad \frac{1}{(1-\Delta r)^{\frac{1}{2}}}, \tag{6}$$

where

$$\bar{M} = \pi\alpha / \sqrt{2}\, G_F = 37.281\ \text{GeV}, \tag{7}$$

and the full correction factor Δr has the value[8]

$$\Delta r = (7.3 \pm 0.8)\ 10^{-2}, \tag{8}$$

for $N_{\text{families}} = 3$ and a reasonable range of values

$$10\ \text{GeV} \leq m_H \leq 1\ \text{TeV}$$
$$20\ \text{GeV} \leq m_t \leq 60\ \text{GeV}. \tag{8'}$$

Notice that, as mentioned earlier, the largest contribution to (8) comes from running the e.m. coupling constant to the weak bosons mass, namely $(6.0 \pm 0.2)\ 10^{-2}$. The variation of the Higgs mass in the range indicated in Eq. (8') has a very tiny effect on Δr ($\sim$O(1%)). This fact is clearly related to the absence of quadratic terms $\sim (m_H^2/m_z^2)$ in the $O(\alpha)$ radiative correction. Indeed one has[6]

$$(\Delta r)_H \sim \frac{11\alpha}{48\pi} \frac{1}{s^2} \ln\left(\frac{m_H^2}{m_z^2}\right), \qquad \text{for } m_H \gg m_z. \tag{9}$$

Quadratic terms are indeed expected to occur in Δr at the two-loop level. However only a very massive Higgs ($m_H \sim 10$ TeV) could make the two-loop effect very sizeable (two-loop $\sim$ one-loop)^2[9].

Deviations of the experimental data from the above result will be a clear indication for new physics. Potentially the largest effect can arise from the possible existence of a new heavy fermion doublet with a large mass splitting[10]. Such a possibility would lead to correct Eq. (6) by a factor

$$R = 1 - \frac{\cos^2\theta_w}{2\sin^2\theta_w} \frac{G_F}{\sqrt{2}} \frac{(\Delta m)^2}{8\pi^2}, \tag{10}$$

where $\Delta m = m_{t'} - m_{b'}$ is the mass splitting of the new heavy family. O(1%) effects require $\Delta m \sim 300$ GeV.

From the above discussion one can draw the following conclusions, before comparing with experiments. A major correction to $M_{z,w}$ ($\sim$ 3%) is simply expected to occur from $\alpha_{e.m.}$ - running. A precision test of the theory at the one-loop level, or possible informations on heavy Higgs's or heavy fermion doublets, can be gained only with measurements at the level of $\delta s^2/s^2 \lesssim 1\%$, which is the accuracy goal to be pursued at LEP[11].

So far the collider data on M_w and M_z are in good agreement with the theoretical predictions. Furthermore the UA2 result[12]

$$\begin{aligned} M_w &= 81.2 \pm 0.8 \pm 1.5 \\ M_z &= 92.4 \pm 1.1 \pm 1.4, \end{aligned} \tag{11}$$

together with (6) leads to

$$s^2 = \left(\frac{38.65}{M_w^2}\right) = 0.227 \pm 0.004 \pm 0.009 \tag{12}$$

to be compared with the recent data[13] from $\bar{\nu}$-deep inelastic scattering:

$$\begin{aligned} s^2 &= 0.227 \pm 0.008 \pm 0.009 \qquad \text{(CD HS)} \\ s^2 &= 0.242 \pm 0.011 \pm 0.005 \qquad \text{(CC FRR)} \end{aligned} \tag{13}$$

The agreement among the various determinations of $\sin^2\theta_W$ is really remarkable and provides also strong support for the standard model. A slightly better precision on the determination of s^2 will be possibly achieved with the improvement programs at the $\bar{p}p$ colliders, including first generation experiments at Fermilab, although for a much more accurate tests of the standard model one has to wait for the operation of e^+e^- colliders.

3. W AND Z PPRODUCTION[14)]

The production of W and Z bosons tests the Drell-Yan mechanism of quark annihilation in a completely new energy regime. The total cross section for vector boson production σ and the rapidity differential cross section $d\sigma/dy$ are predicted by the QCD improved parton model[15)] as an expansion in the strong soupling constant α_s. The corrections of order α_s to these cross-sections have been calculated and found to be important[16)]. They increase the naive parton model prediction by an energy and rapidity dependent factor, commonly referred to as the "K-factor". At fixed target energies the $O(\alpha_s)$ corrections are dangerously big and resummation techniques must be invoked[17)] in an attempt to control the perturbation series. At collider energies their size is reduced because the coupling constant is smaller and, for the production of weak intermediate bosons, they lead to a correction of about 30%. The total cross-section is therefore more reliably predicted by perturbation theory at these energies with a smaller theoretical error on the overall normalizazion.

The relevant formulae are given here for the case of Drell-Yan pairs, of Z and W production

$$Q^2 \frac{d\sigma^{\gamma^*}}{dQ^2} = \frac{4\pi\alpha^2}{9S} K \sum_f e_f^2 \int dx_1 dx_2 \, \delta(x_1 x_2 - \tau) \left\{ q_f(x_1, Q^2)\bar{q}_f(x_2, Q^2) + (1 \leftrightarrow 2) \right\} \quad (14a)$$

$$\sigma^Z = \frac{\pi^2 \alpha}{12 \sin^2\theta_W \cos^2\theta_W} \frac{K}{S} \sum_f n_f^Z \cdot$$

$$\cdot \int dx_1 \, dx_2 \, \delta(x_1 x_2 - \tau) \left\{ q_f(x_1, Q^2) \, \bar{q}_f(x_2, Q^2) + (1 \leftrightarrow 2) \right\}, \quad (14b)$$

$$\sigma^W = \frac{\pi^2 \alpha}{3 \sin^2\theta_W} \frac{K}{S} \int dx_1 \, dx_2 \, \delta(x_1 x_2 - \tau) \cdot$$

$$\cdot \left\{ u(x_1, Q^2) \, \bar{d}(x_2, Q^2) \cos^2\theta_C + u(x_1, Q^2) \, \bar{s}(x_2, Q^2) \sin^2\theta_C + \ldots \right\}, \quad (14c)$$

where $\tau = Q^2/S$ ($Q^2 = M^2$ for the weak bosons), e_f are the quark charges, n_f^Z the coupling of

the Z boson to the quarks $n_f^Z=(1-(4/e_f)/\sin^2\theta_W)^2+1$ and $K\equiv K(Q^2,\tau)$ is the K-factor[18]. The other notations are standard.

The choice of the parton densities does not affect sizeable the accuracy of the theoretical predictions. Indeed in the energy range actually covered by experiments the parton densities are probed at values $x_{1,2}\sim\sqrt{\tau}\sim 0.15$, where the valence quark distributions are quite well known from deep inelastic data. Other sources of theoretical uncertainties are the scale Q^2 appearing in the parton distributions and in α_s and the value of Λ. One could argue in fact that the relevant scale Q^2 could be of order $<q_T^2>$ instead of $M^2_{W,Z}$, where $<q_T>$ is the average transverse momentum ($<q_T>\sim 8$ GeV).

The theoretical predictions[19,20] at $\sqrt{s}$=540 and 630 GeV, compared with the experimental results[12, 21,22], are given by

$\sigma^W B(W\to e\nu)$	UA1	UA2	$\sqrt{s}$ (GeV)	
$370\ ^{+110}_{-\ 60}$	$530\pm 80\pm 90$	$500\pm 100\pm 80$	540	(15a)
$470\ ^{+140}_{-\ 80}$	$480\pm 40\pm 80$	$540\pm 70\pm 90$	630	

and

$\sigma^Z B(Z\to e\bar{e})$	UA1	UA2	$\sqrt{s}$	
$42^{+12}_{-\ 6}$	$41\pm 21\pm 7$	$101\pm 37\pm 15$	540	(15b)
$51^{+16}_{-\ 9}$	$64\pm 21\pm 10$	$56\pm 20\pm 9$	630	

where the cross sections are expressed in pb and the leptonic branching ratios are assumed to be $\Gamma(W\to e\nu)=0.089$ and $\Gamma(Z\to e\bar{e})=0.032$.

Eqs. (15) clearly show agreement between theory and experiments. Notice that if $O(\alpha_s)$ corrections were not included the theoretical estimates had to be lowered by $\sim$ 30% leading to a quite uncomfortable situation, barely compatible with the experimental errors.

The prediction of the boson transverse momentum distribution is more subtle, since all order effects need to be taken into account. Renormalization group improved perturbation theory is valid when the transerve momentum q_T is of the same order as the vector boson mass Q. The large q_T tail of the transverse momentum distribution was one of the early predictions of the QCD improved parton model[23]. As q_T becomes less than Q, such that $\Lambda \ll q_T \ll Q$, a new scale is present in the problem and large terms of order

$$\frac{1}{q_T^2}\,\alpha_s^n\,(q_T^2)\,\ln^m(Q^2/q_T^2), \qquad (m\leq 2n-1)$$

occur, forcing the consideration of all orders in n. These terms are characteristic of a theory with massless vector gluons. Fortunately, in the leading double logarithmic approximation (DLA:m=2n-1) these terms can be reliably resummed. This resummation was

first attempted by Dokshitzer-Diakonov-Troyan (DDT)[24] and subsequently modified and consolidated[25]. A consistent framework for going beyond the leading double logarithmic approximation has been developed and a complete picture has begun to emerge[26]. The resulting cross sections allow a precise test of the theory in the region $q_T \ll Q$. Of course, at very small q_T ($q_T \sim \Lambda$) non-perturbative effects also become important. For the first generation of Drell-Yan experiments is was difficult to separate clearly the regions $q_T \sim \Lambda$, $\Lambda \ll q_T \ll Q$ and $q_T \sim Q$. At the $p\bar{p}$ collider the observation of the weak bosons q_T distributions gives a unique opportunity to test these theoretical ideas.

In a recent paper[19] the problem of q_T distributions in Drell-Yan processes has been reexamined. The large amount of theoretical information accumulated in recent years has been included in a systematic way. The final expression for the q_T distribution satisfies the following requirements:

(a) At large q_T, we automatically recover the $O(\alpha_s)$ perturbative distribution coming from one-gluon emission, without the ad hoc introduction of matching procedures between hard and soft radiation.

(b) In the region $q_T \ll Q$ the soft gluon resummation is performed at leading double logarithmic accuracy. The role of subleading terms in the summation is also evaluated.

(c) Only terms corresponding to the emission of soft gluons, for which the exponentiation can be theoretically justified, are resummed.

(d) The integral of the q_T distribution reproduces the known results for the $O(\alpha_s)$ total cross-section (i.e., including the "K-factor").

(e) The average value of q_T^2 is also identical with the perturbative result at $O(\alpha_s)$.

(f) All quantities are expressed in terms of precisely defined quark distribution functions at a specified scale as for example those determined by the deep inelastic structure function F_2 at the scale Q^2.

The form of the result is

$$\frac{d}{dq_T^2\, dy} = N \int \frac{d^2b}{(2\pi)^2}\, e^{-\vec{b}\vec{q}_T} \left[R(b^2,Q^2)\exp S(b^2,Q^2)\right] + Y(q_T^2,Q^2) \qquad (16)$$

where the Sudakov form factor (including only terms which can deduced from an $O(\alpha_s)$ calculation), is

$$S(b^2,Q^2) = \int_0^{A_T^2} \frac{d\mu^2}{\mu^2} \left[J_o(b\mu)-1\right] \frac{4}{3} \frac{\alpha_s(\mu)}{2\pi} (2 \ln \frac{Q^2}{\mu^2} - 3). \qquad (17)$$

The complete $O(\alpha_s)$ expressions for Y and R are given in Ref. 19) and are too complicated to reproduce here. The zeroth order term in R involves the parton distribution functions evaluated a b-dependent scale

$$R \sim q(x_1^o,B^2)\, \bar{q}\,(x_2^o,B^2) + O(\alpha_s)\,, \qquad B^2 \sim 1/b^2$$

with $\tau = M^2/S$, $x^o_{1,2} = \sqrt{\tau}\exp(\pm y)$, and $A_t^2 = \left[(S+Q^2)^2/4S\cosh^2 y - Q^2\right]$ is the kinematical bound of the transverse momentum squared for gluon emission. The function Y is completely finite as q_T tends to zero.

The bulk of the q_T distribution, where most of the data have been collected, comes from the soft part of Eq. (16). Of course the residual finite terms play a major role for large q_T, say $q_T \gtrsim 30$ GeV where Eq. (16) tends to the $O(\alpha_s)$ perturbative result. The so called "leading approximation", where one keeps only the logarithmic $\ln(Q^2/\mu^2)$ in Eq. (17) gives a very poor description of the weak boson distribution and consequently of the decay lepton spectrum.

The numerical consequences of Eq. (16) are shown in Fig. 1 with histograms of the

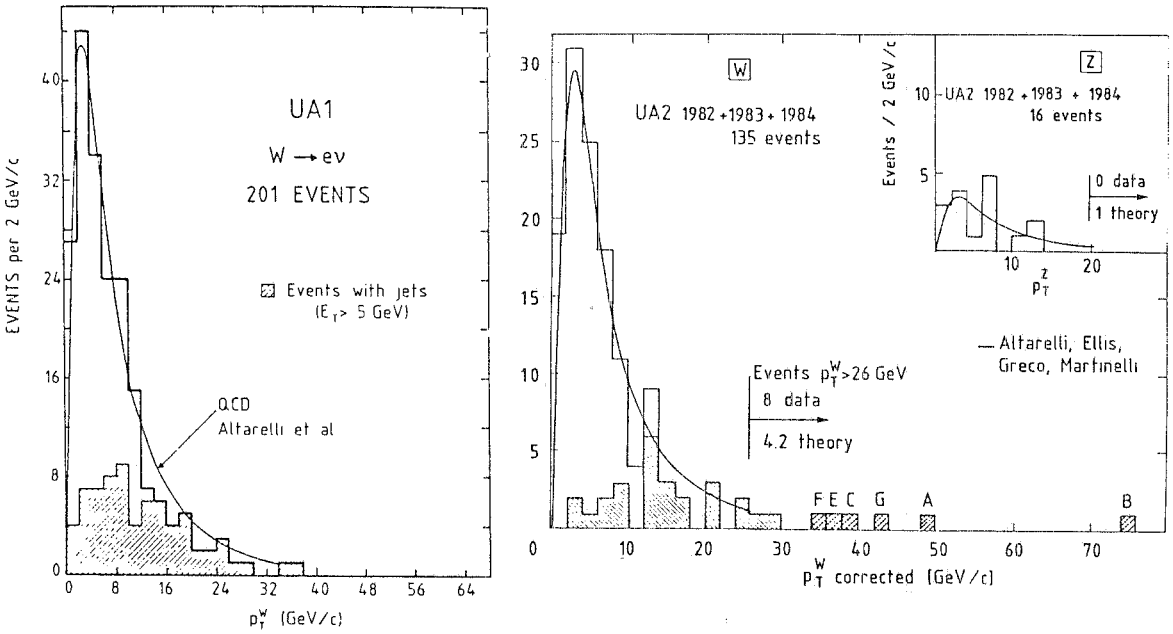

FIG. 1

UA1[22] and UA2[27] W events suitably normalized. The principal uncertainties in Eq. (16) are associated with the choice of Λ. This leads to a variation of about 15%, as shown in Fig. 2. The form of the parton distribution function leads to a small uncertainty, since quark distributions, well determined in deep inelastic scattering, are most important.

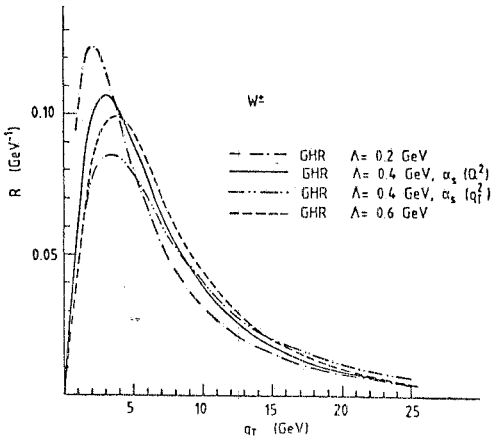

FIG. 2

The general structure of Eq. (16) has been recently checked[28] in a recent calculation to order (α_s^2). Writing Eq. (17) in a more general form

$$S(b^2,Q^2) = \int \frac{d\mu^2}{\mu^2} \left[J_o(b\,\mu)-1\right] \left[\ln\left(\frac{Q^2}{\mu^2}\right) A(\alpha_s) + B(\alpha_s)\right] \qquad (18)$$

with

$$A(\alpha_s) = \sum_i \left(\frac{\alpha_s}{2\pi}\right)^i A^{(i)}, \qquad B(\alpha_s) = \sum_i \left(\frac{\alpha_s}{2\pi}\right)^i B^{(i)}.$$

the new calculation confirms the previous result[29] for $A^{(2)}$ and also determines $B^{(2)}$. Numerically the additional corrections are of order of $A^{(1)}$ and $B^{(1)}$ and therefore not more important than the uncertainties associated with the choice of the scale Λ.

The exact knowledge of the large q_T tail of the distribution is crucial for an accurate determination of the level of the QCD background to possible new physics.

Typical examples of background are the monojet events coming from $q\bar{q} \rightarrow$ Z,W+ hard gluon, with $Z \rightarrow \nu\bar{\nu}$ ($\Gamma(Z \rightarrow \nu\bar{\nu}) \simeq 6\ \Gamma(Z \rightarrow e\bar{e})$) or $W \rightarrow \ell\nu$ (ℓ undetected lepton). Then it is useful to define[20] $\pi(q_T)$ as the probability of producing W/Z with a transverse momentum larger than q_T, i.e.

$$\pi(q_T) = \frac{\int_{q_T}^{q_{T\max}} \left(\frac{d\sigma}{d\,q_T}\right) d\,q_T}{\int_{o}^{q_{T\max}} \left(\frac{d\sigma}{d\,q_T}\right) d\,q_T}, \qquad (19)$$

which, for $q_T \gtrsim 25$ GeV, is essentially determined by the $O(\alpha_s)$ perturbative contribution. The figures presented in Table I[20], clearly show that a few standard model events with missing E_T are expected to accompany the W and Z sample collected so far. A fully quantitative study[30] of this question, in terms also of the kinematical cuts applied in the experiments, indicates that an expected members of (6^{+5}_{-2}) monojet events with $E_T^{miss} > 40$ GeV is associated to the actual W (~ 200 events) and Z (19 events) samples, clearly compatible with the present observations.

The observation of jets produced in association with vector bosons allows for an explicit test of perturbation theory leading also to a direct measurement of α_s. From a theoretical point of view, this is a much cleaner problem than for the analogous case in pure jet physics (three jets/two jets, see next section), where the very large number of real and virtual Feynman diagrams ($O(10^3)$) contributing to the observed n-jets ($n \geq 2$) final state, prevents a simple answer. A few remarks however are in order to clarify the dependence of this type of α_s measurement upon the jet detection criteria.

TABLE I

q_T	$\pi^W(q_T)\%$	$\pi^Z(q_T)\%$
25	4.4 ± 2.0	5.1 ± 2.5
30	2.7 ± 1.1	3.2 ± 1.3
35	1.7 ± 0.7	2.0 ± 0.8
40	1.1 ± 0.4	1.4 ± 0.5
45	0.7 ± 0.3	0.9 ± 0.3
50	0.5 ± 0.1	0.6 ± 0.2
55	0.30 ± 0.07	0.40 ± 0.10
60	0.20 ± 0.07	0.25 ± 0.10

$\sqrt{S}$ =540 GeV.

q_T	$\pi^W(q_T)\%$	$\pi^Z(q_T)\%$
25	5.4 ± 2.3	6.1 ± 2.8
30	3.5 ± 1.3	4.0 ± 1.6
35	2.3 ± 0.8	2.6 ± 1.0
40	1.5 ± 0.5	1.8 ± 0.6
45	1.0 ± 0.3	1.2 ± 0.4
50	0.7 ± 0.2	0.9 ± 0.2
55	0.50 ± 0.15	0.60 ± 0.15
60	0.30 ± 0.09	0.40 ± 0.12

$\sqrt{S}$ = 630 GeV.

In principle one can write[31]

$$\sigma_{tot}(W,Z) = \sum_{n=0}^{\infty} \sigma_n(W,Z + n \text{ jets}), \tag{20}$$

where σ_n clearly depends on the jet identification criteria.

Indeed, expanding Eq. (20) in power of α_s, one gets schematically:

$$\sigma_{tot} = \sigma_o + \sigma_1 \alpha_s(Q^2) + \sigma_2 \alpha_s^2(Q^2) + \ldots \tag{21}$$

with

$$\sigma_1 = \sigma_1^D + (\sigma_1^V + \sigma_1^U)$$

$$\sigma_2 = \sigma_2^{DD} + (\sigma_2^{DU} + \sigma_2^{DV}) + (\sigma_2^{UU} + \sigma_2^{UV} + \sigma_2^{VV})$$

and so on. The labels V, D and U stand for virtual, real and detectable, real and not detectable gluons respectively, according to a given experiment. Then Eq. (21) can be rewritten, as

$$\begin{aligned}\sigma_{tot} = &\left\{\sigma_o + \alpha_s(\sigma_1^V + \sigma_1^U) + \alpha_s^2(\sigma_2^{UU} + \sigma_2^{UV} + \sigma_2^{VV}) + \ldots\right\} \\ &+ \alpha_s\left\{\sigma_1^D + \alpha_s(\sigma_2^{DU} + \sigma_2^{DV}) + \ldots\right\} + \alpha_s^2\sigma_2^{DD} + \ldots \\ &\equiv \sigma_o K_o + \alpha_s\sigma_1^D K_1 + \alpha_s^2\sigma_2^{DD} K_2 \ldots,\end{aligned} \tag{22}$$

The appearance of the factor $K_n = 1 + O(\alpha_s)$ multiplying the cross section for n-detected jets produced in association with the weak bosons, thus prevents a naive extractions of α_s from the measured ratio $\sigma_n^{meas} / \sigma_{n-1}^{meas}$.

Jet multiplicity distributions for hadronic jets produced in association with W's and Z are shown in Figs. 3-4 for UA1[22] and UA2[27] respectively. The result of a recent analysis[31] which extensively discusses the theoretical basis for partitioning the cross section into n-jet contributions and the role of K factors is shown in Fig. 5, together with the theoretical uncertainties and a comparison with UA1 data. Clearly there is agreement between theory and experiments.

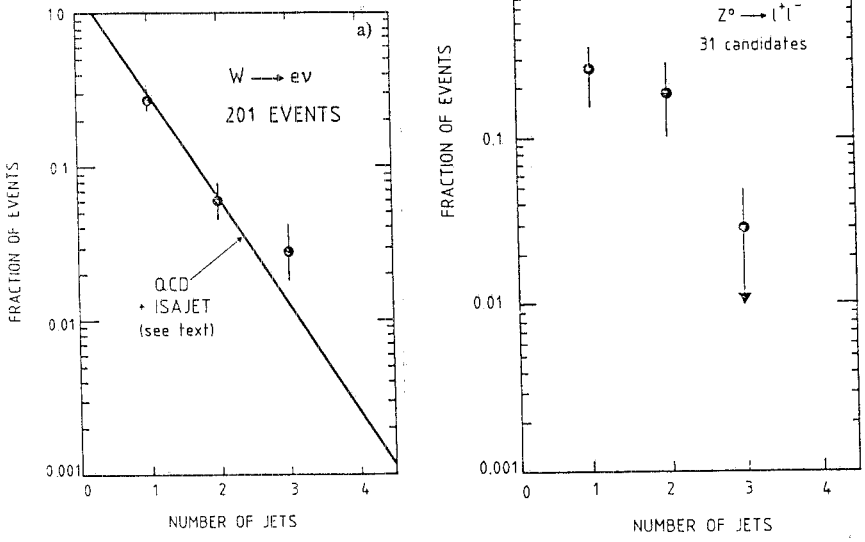

FIG. 3

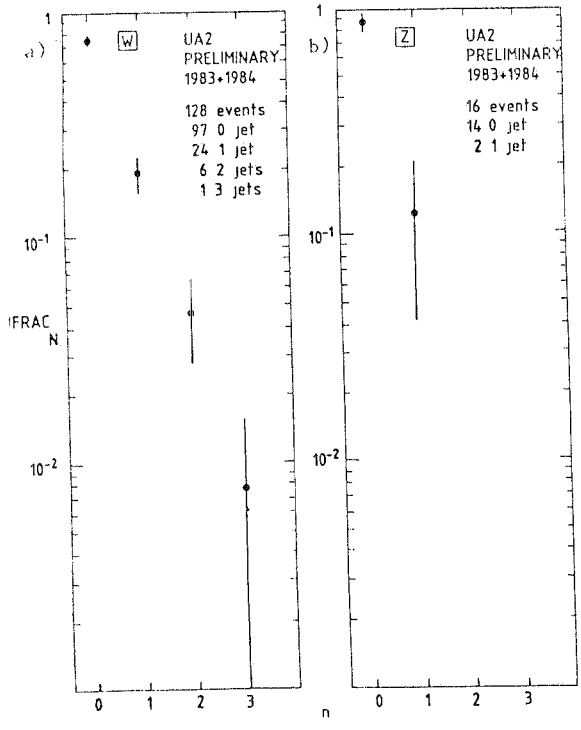

FIG. 4

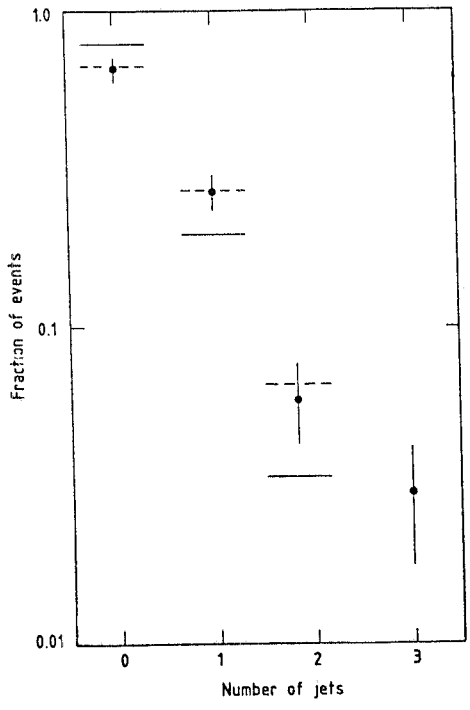

FIG. 5

All the above results concerning W's and Z production show a very good agreement of collider data with perturbative QCD. The q_T distributions, in particular, have provided an important test of the theory well beyond the lowest order expansion in α_s.

4. JET PHENOMENA[14)]

Jets have long been expected[32)] to appear as clear evidence for the parton substructure of the hadrons. They have been first observed[33)] at the highest ISR energies ($\sqrt{s} \gtrsim 50$ GeV) but have been unambigously produced at $S\bar{p}pS$ collider[1,34,35)] with a production cross section a few orders of magnitude bigger and p_T up to ~ 100 GeV.

The jet yield is calculated using the improved parton model formula

$$d\sigma(a+b \to c+X) = \sum_{ij} \int_0^1 dx_1 dx_2 f_i^{(a)}(x_1,Q^2) f_j^{(b)}(x_2,Q^2) d\hat{\sigma}\ (ij \to cX), \qquad (23)$$

where the sum runs over different types of partons, $d\hat{\sigma}$ is the subprocess differential cross section, and the structure functions are considered to a scale Q^2 of order p_T^2. The exact appropriate scale ($Q^2 \sim p_T^2$, $p_T^2/4$, ...) can be fixed only after computation of next to leading terms.

More generally, it is useful to introduce[36)] the concept of differential luminosity of parton-parton collisions at a given c.m. energy $\sqrt{s}$ of the colliding partons:

$$\tau \frac{d\mathscr{L}^{ij}}{d\tau} = \frac{\tau}{(1+\delta_{ij})} \int_\tau^1 \frac{dx}{x} \left[f_i^{(a)}(x)\, f_j^{(b)}\left(\frac{\tau}{x}\right) + f_j^{(a)}(x)\, f_i^{(b)}\left(\frac{\tau}{x}\right) \right], \qquad (24)$$

where $\tau = \hat{s}/s$, with $\sqrt{s}$ the c.m. energy of collider hadrons a and b. This differential luminosity represents the number of parton-parton collisions with scaled c.m. energies in the interval $(\tau,\ \tau+d\tau)$ per hadron-hadron collision. Then for the hadronic reaction (23) one obtains, for example,

$$\frac{d\sigma}{d\tau}(ab \to c+X) = \sum_{ij} \tau \left(\frac{d\mathscr{L}^{ij}}{d\tau}\right) \hat{\sigma}(ij \to c). \qquad (25)$$

The parton-parton luminosity measures therefore the relative importance of a given combination of partons for a fixed beam type. Of course the cross section $\hat{\sigma}(\hat{s}) \sim c/\hat{s}$ weights further the contribution of a given subprocess to the hadronic reaction df interest. As an illustration we plot in Figs. 6[36)] the quantity $(\tau/\hat{s})(d\mathscr{L}/d\tau)$, which has dimensions of a cross section as a function of $\sqrt{\hat{s}}$, for total c.m. energies ranging between 2 and 100 TeV. They correspond respectively to the gg, qg and qq contributions in pp collisions, or similarly, gg, $q(\bar{q})g$ and $q\bar{q}$ in $p\bar{p}$ collisions. The luminosities are based upon the parton distribution of Ref. 36). By direct comparison of Figs. 6 it is quite clear the dominance of gluon interactions at $\sqrt{\hat{s}} \lesssim 0.1$ TeV and $\sqrt{s} \sim 1$ TeV. This fact, together with the large

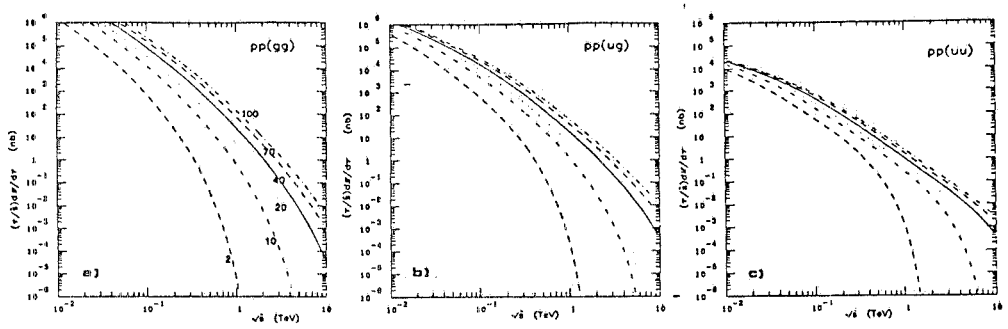

FIG. 6

gluon cross sections discussed below, gives to the Sp$\bar{p}$S collider quite a good chance to first reveal the manifestation of the non-Abelian character of the theory.

To lowest order QCD the parton-parton cross sections are given[37]

$$\frac{d\sigma}{d\hat{t}} = \pi \frac{\alpha_s^2(Q^2)}{\hat{s}^2} \left| A(\hat{s}, \hat{t}, \hat{u}) \right|^2 , \qquad (26)$$

where $\hat{s}$, $\hat{t}$, $\hat{u}$ are the usual Mandelstam variables and $\left| A(\hat{s}, \hat{t}, \hat{u}) \right|^2$ is indicated in Table II for nine different subprocesses, with its numerical value at 90° in the parton parton centre

TABLE II - Parton cross-sections: $d\sigma/dt=(\pi\alpha^2/s^2)|M|^2$ [averaged (summed) over initial (final colours and spins]. s, t, u refer to the parton processes. F_M is the value of $|M|^2$ at c.m. angle $\theta=90°$ (s:t:u=4:-2:-2).

PARTON PROCESS	$\|M\|^2$	F_M
$q\bar{q}' \to q\bar{q}'$ $qq' \to qq'$	$\frac{4}{9}\frac{s^2+u^2}{t^2}$	2.22
$qq \to qq$	$\frac{4}{9}(\frac{s^2+u^2}{t^2} + \frac{s^2+t^2}{u^2}) - \frac{8}{27}\frac{u^2}{st}$	3.26
$q\bar{q} \to q'\bar{q}'$	$\frac{4}{9}\frac{t^2+u^2}{s^2}$	0.22
$q\bar{q} \to q\bar{q}$	$\frac{4}{9}(\frac{s^2+u^2}{t^2} + \frac{t^2+u^2}{s^2}) - \frac{8}{27}\frac{u^2}{st}$	2.59
$q\bar{q} \to gg$	$\frac{32}{27}\frac{u^2+t^2}{ut} - \frac{8}{3}\frac{u^2+t^2}{s^2}$	1.04
$gg \to q\bar{q}$	$\frac{1}{6}\frac{u^2+t^2}{ut} - \frac{3}{8}\frac{u^2+t^2}{s^2}$	0.15
$qg \to qg$	$-\frac{4}{9}\frac{u^2+s^2}{us} + \frac{u^2+s^2}{t^2}$	6.11
$gg \to gg$	$\frac{9}{2}(3 - \frac{ut}{s^2} - \frac{us}{t^2} - \frac{st}{u^2})$	30.4

of mass. On the basis of these parton cross sections it is clear that processes involving initial state gluons are largerly favoured also due to colour factors.

Experimentally, events with two clear wide angle jets dominate the background when requiring a sufficiently large amount of transverse energy ($E_T \gtrsim 100$ GeV). Then one has been able to test various predictions of QCD, in spite of the uncertainties associated to the theory, mainly coming from the choice of the scale Q^2, the parametrization of the structure functions and the higher order corrections, as discussed later.

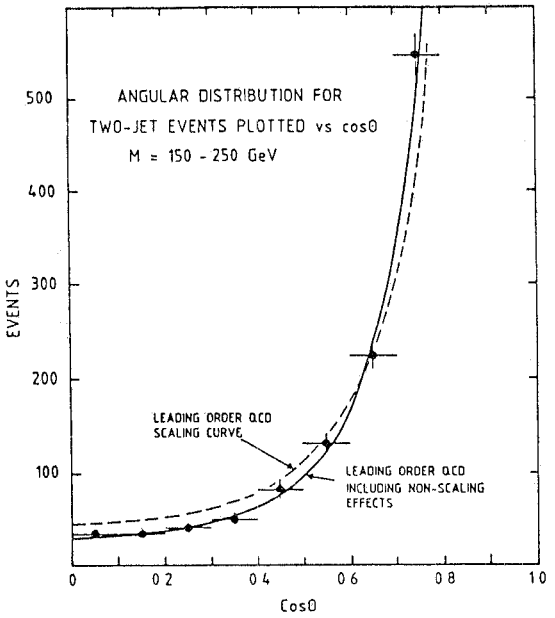

FIG. 7 - The angular distribution for two-jet events plotted versus cos θ, the c.m. scattering angle, for M_{2J} = 150-250 GeV and cos θ < 0.8. The data are from UA1 (Ref. 38).

First the jet angular distribution has been found very indicative of vector exchange in parton scattering. The corresponding (sin $\theta^*/2)^4$ behaviour is shown[38] in Fig. 7. Notice the very good experimental accuracy which allows to detect clearly the presence of non scaling effects.

The inclusive jet yield measured by UA2[39] is compared in Fig. 8 with the absolute

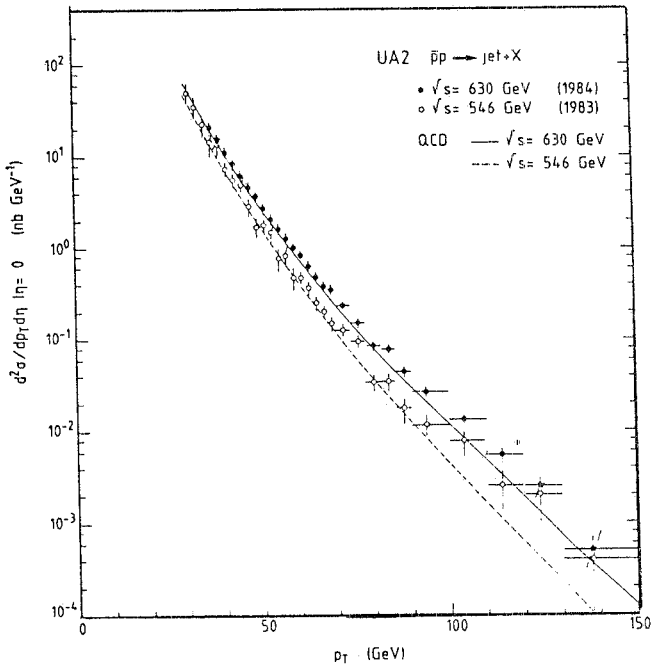

FIG. 8

QCD prediction obtained by using the structure functions parametrization of Ref. 36). The theoretical uncertainty is little affecting the shape of the curve and could mainly change the overall scale by a factor 2-3. The sources of uncertainty are related to the value of Λ, to the scale Q^2 in α_s and in the parton densities and to higher order corrections (K-factors). For example, assuming $Q^2 = q_T^2/4$, one simply gets $\left[\alpha_s^2(\Lambda=0.5)/\alpha_s^2(\Lambda=0.1)\right]_{p_T \gtrsim 20\ \mathrm{GeV}} \lesssim 2.5$. Furthermore the complete calculation of $O(\alpha_s^3)$ corrections to the $(2 \rightarrow 2)$ subprocesses is still missing because of its complexity, expecially in the case of gluon-gluon scattering. Some very special terms of soft origin have been identified[40], similarly to the π^2 term in the Drell-Yan K factor, but the full computation is far from being completed. This lack of information is also at the origin of the ambiguity of the choice of the scale Q^2 in the parton densities and in the running coupling constant. The only suggestion we have, i.e. $Q^2=p_T^2/4$, comes from the calculation[41] of the reaction $q_i+q_j \rightarrow q_i+q_j+g$. On the other hand the theoretical prediction is not very sensitive to our poor knowledge of the gluon distribution function. In fact, despite possible large differences at low Q^2, various gluon densities become practically identical at the scale relevant for high p_T jets, as illustrated[42] in Fig. 9.

We have so far limited our discussion to jet production to order α_s^2. The production of three well separated jets at large p_T clearly corresponds to the $O(\alpha_s^3)$ perturbative description of $(2 \rightarrow 3)$ parton subprocesses. The full calculation of such terms has been performed[43] and the results can be cast[44] in

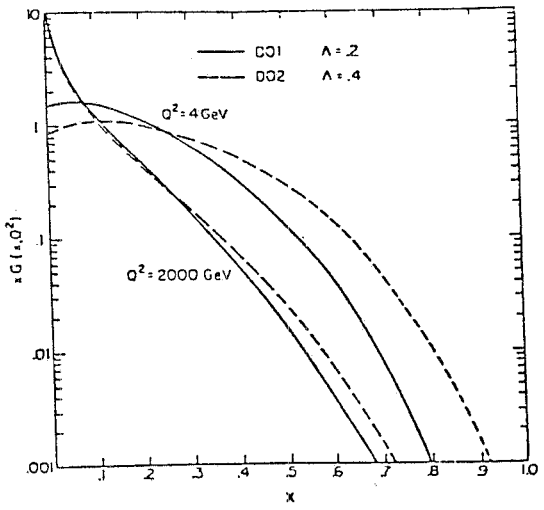

FIG. 9

a suggestive simple form, which seems to generalize the well known factorization of infrared singularities in the soft limit. It reads (p_i, p_j, ... are generic partons)

$$\sigma(p_i+p_j \rightarrow p_k+p_l+g) = \left|M\right|^2 I, \qquad (27)$$

where $\left|M\right|^2$ and I approach the non radiative section $\left|M_0\right|^2$ and the infrared factor respectively when the momentum k_g of the additive gluon vanishes. Of course those results are only valid away from the regions of soft and collinear singularities.

Easy tests of three jet production are obtained by looking at various distributions characteristic of bremsstrahlung processes. In Fig. 10 the three jet angular distribution is plotted[38] for the variable ψ, defined as the angle between the plane containing jet-2 and jet-3 and the plane containing jet-1 and the incoming parton (the final jets relative energies

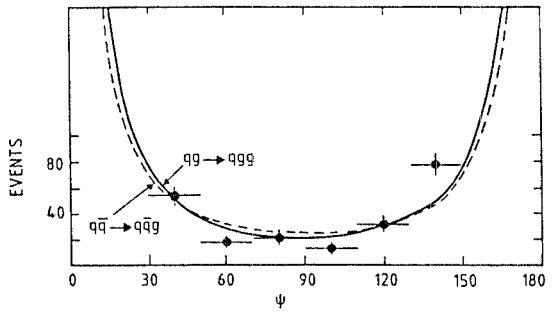

FIG. 10

x_i, i=1,2,3, are ordered such that $x_1 > x_2 > x_3$). The ψ-distribution exhibits forward-backward peaking. This arises because the preferred configuration occurs when jet-2 and jet-3 lie in the plane containing jet-1 and the incoming partons (ψ=0° and ψ=180°).

Fig. 11 displays[39] the acoplanarity angle $\emptyset$ distribution for three-jet event in an angular region where the two-jet contribution is negligible. A QCD computation[45] for three-parton final states (full line) and a calculation assuming a pure three-parton phase space (dashed line) are also presented in the same figure. The phase space prediction is certainly ruled out and this is a good indication of the sensitivity of this variable to QCD effects.

Finally Fig. 12, shows[39] the p_T^{out} distribution compared with the results of the predictions of Ref. 45) for three parton final states normalized to the two-jet sample.

The clear evidence for three-jet production and the agreement with leading order QCD predictions has led the UA1 and UA2 collaborations to extract α_s from the relative rate of the three-jet and two-jet events[38,39]. It should be noted however that there is a

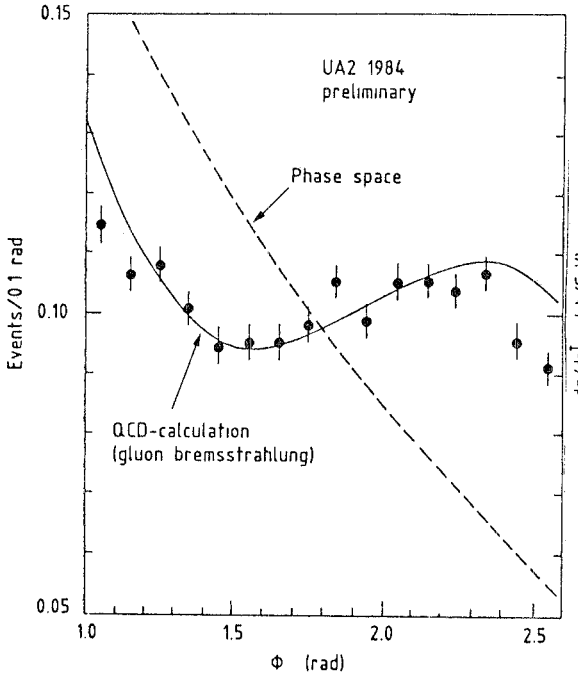

FIG. 11

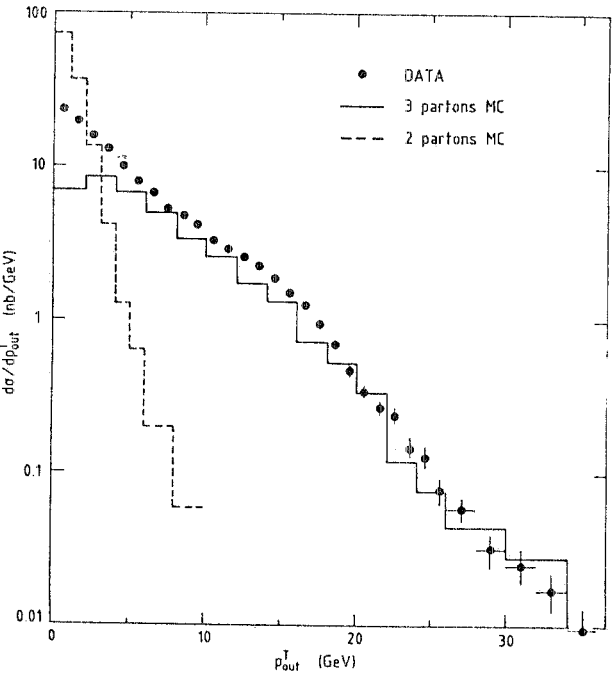

FIG. 12

considerable theoretical ambiguity associated to this procedure of estimating the values of α_s.

Indeed, from the previous discussion on $\sigma(W,Z + n \text{ jets})$ in the preceding section, from the absence of a complete calculation of the relevant K-factor and the dependence on the hadronization models which are used to define the jets in a given experiment, it follows that the above α_s determination is strongly affected by systematic uncertainties which are difficult to be estimated quantitatively.

Finally let us discuss some characteristic features of gluon jets, which are expected to dominate the hadronic final states, as mentioned earlier, and compare them with the corresponding phenomena for quark jets. As well known, perturbative QCD predicts striking differences between quark and gluon jets occurring in various kinematical distributions, like transverse momentum or rapidity, in the multiplicities and other jet fragmentation properties, owing to the different colour structure of the basic diagrams. Progress has been recently made in this direction, including the study of next-to-leading corrections, trying in particular to isolate genuine gluon effects, from pure phenomenological hadronization models. The recent data are quite consistent with QCD expectations, as discussed below for some cases.

First the effect of the three gluon coupling has been revealed directly by looking at the transverse momentum unbalance of the two almost back-to-back jets, as the result of bremsstrahlung from the initial gluon legs[46]. Due to the dominance of gluon-gluon and quark-gluon scattering at the collider the resulting p_T^{ij} distribution is quite sensible to non-Abelian colour factor $C_A(C_A=3)$, to be contrasted to the case of the weak bosons p_T distribution, which essentially depends on the quark gluon coupling C_F $(C_F=4/3)$. Experimentally, p_T^{ij} is the vector sum of two large and opposite momenta and is therefore sensitive to instrumental effects. The two components p_η^{ij} (along the bisector of the two jets in the transverse plane) and p_ζ^{ij} (orthogonal to it and roughly parallel to the two-jet axis) are studied separately, because they are associated with different resolution and systematic effects.

Then the p_ζ^{jj}-p_η^{jj} distributions are shown[47] in Fig. 13, compared with the theoretical predictions[46]. The calculated spectrum (dashed line) is transformed into the histogram when one takes into account detector smearing. Also shown is the expectation (dashed-dotted line) in the hypothetical case where gluons and quarks were to radiate the same way. The close agreement between the expectations and data is a clear evidence for the non-Abelian structure of the theory.

The study of the internal transverse momentum within the jet also fits the expectation than gluon jets are broader than quark jets. This is shown[48] in Fig. 14 where the ratio of the p_T distributions between "pure" samples of gluon and quark jets is plotted. The distinction between quark and gluon jets is made by defining a corresponding probability based on the knowledge of the structure functions and the parton-parton cross sections.

FIG. 13

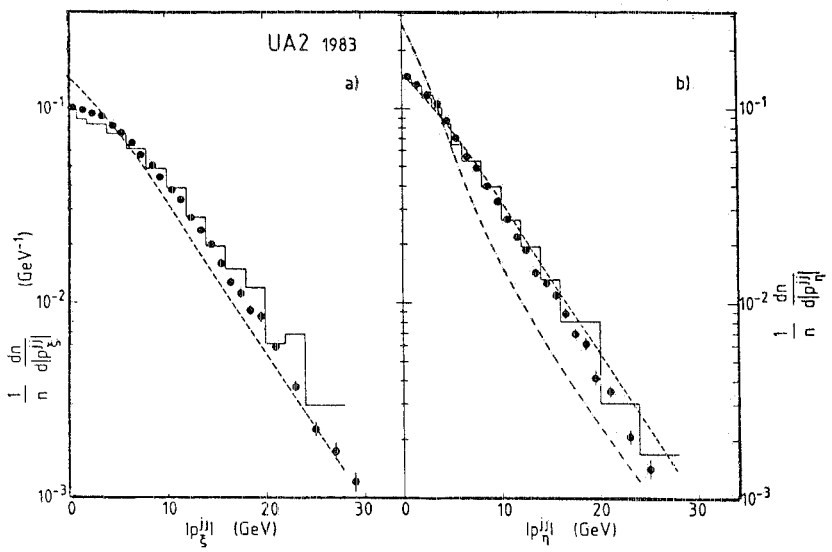

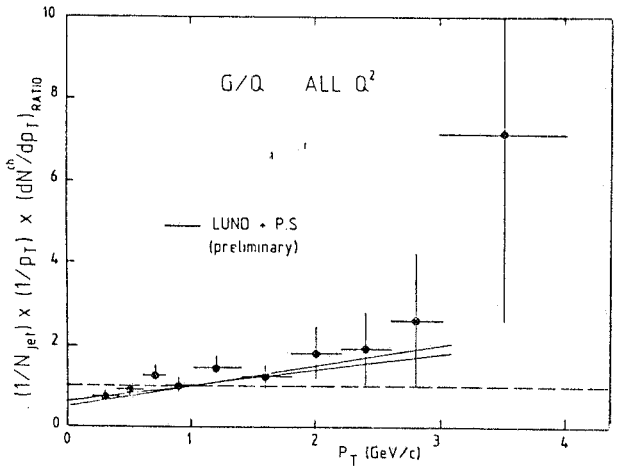

FIG. 14 - Ratio between "pure" gluon and quark internal p_T distributions. The data are from UA1 (Ref. 48).

Inclusive fragmentation functions[47] and multiplicity distributions[49] have also been studied and compared will e^+e^- data. The results are qualitatively consistent with the expectations, although the experimental evidence for the difference between quark and gluon jets is not so striking in these cases[50]. It should be stressed that the full explanation of the jet fragmentation is not at present a fundamental test of QCD because of the relevance of non-perturbative effects in the hadronization phase of the jet development.

In summary, the study of jet physics at the $Sp\bar{p}S$ collider is becoming very sophisticated. The intensive jet production at large p_T, with the dramatic importance of gluon effects, gives clear evidence in favor of perturbative QCD. A complete computation of the $O(\alpha_s^3)$ corrections is however necessary for a full quantitative agreement with data.

Before closing this section, I would like to add a comment on Higgs boson production in gluon-gluon collisions. For $M_H \leq 2M_W$ the gluon fusion mechanism has been suggested[51] as a very promising source of Higgs bosons in hadron collisions. The subsequent decay into the heaviest accessible pair of quarks would lead to a significant signal in the jet-jet cross section. However it has been observed[52] that the gluon fusion reaction $gg \rightarrow H \rightarrow Q\bar{Q}$

actually adds to the direct QCD process $gg \rightarrow Q\bar{Q}$, interfering clearly with it. Then for $M_H > 2M_Q$ the resulting <u>total</u> cross section possesses a peculiar shape typical of an interference process. This is shown in Fig. 15, obtained in Ref. 52 for M_H=100 GeV and

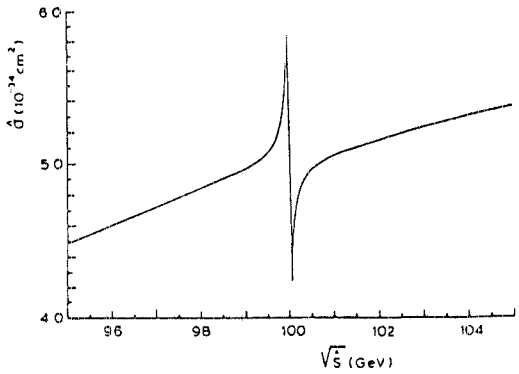

<u>FIG. 15</u> - Cross section as a function of gg c.m. energy.

m_t=40 GeV. The width of the Higgs boson Γ_H, which determines the interference pattern, is typically of the order of 50-100 MeV. From this result one could draw the conclusion order to reveal the Higgs boson via this mechanism one would need an extremely good resolution in the $b\bar{b}$ or $t\bar{t}$ jet-jet invariant mass.

However, due to initial state gluon bremsstrahlung the jet-jet system is actually produced with an effective transverse momentum imbalance of order $\langle k_T^2 \rangle$, which corresponds to an "intrinsic" resolution in the parton c.m. energy squared $\Delta\hat{s} \sim \langle k_T^2 \rangle$ [46]. This radiation effect, with a proper width much larger than Γ_H, automatically leads to an effective cross section which is quite insensitive to the production of the Higgs boson [53]. Therefore the eventual existence of the Higgs with $M_H \sim 100$ GeV, cannot be revealed through this production and decay mechanism, unless the Higgs boson couplings differ from those expected in the standard model.

The work reported here has been the result of very stimulating and enjoiyable discussions with many colleagues at the St. Vincent Workshop. I would also like to thank Prof. Jacob Grunhans and his colleagues for organizing this excellent meeting in such a beautiful country.

REFERENCES

1) Proc. of the 4th Topical Workshop on Proton-Antiproton Collider Physics, Bern (1984).
2) Proc. of the 5th Topical Workshop on Proton-Antiproton Collider Physics, St. Vincent (1985).
3) S.L. Glashow, contr. to (2); R.F. Schwitters, contr. to (2).
4) For further details see also: W.J. Marciano, contr. to (1); L. Maiani, University of Rome Preprint - N.I. 841, (1985); M. Consoli, contr. to (2); G. Altarelli, LEP Jamboree, CERN, March 1985.
5) S.L. Glashow, Nucl. Phys. 22, 579 (1961); S. Weinberg, Phys. Rev. Lett. 19, 1264 (1967); A. Salam, in Proc. of the 8th Nobel Symposium ed. N. Svartholm (Almquist and Wiksell, Stockholm 1968), p. 367.
6) A. Sirlin, Phys. Rev. D22, 971 (1980); W. Marciano and A. Sirlin, Phys. Rev. D22, 2695 (1980).
7) A. Sirlin, Phys. Rev. D29, 89 (1984).
8) M. Consoli, contr. to (2).
9) J.van der Bij and M. Veltman, Nucl. Phys. B231, 205 (1984).
10) M. Veltman, Nucl. Phys. B123, 89 (1977).
11) G. Altarelli, ref. 4).
12) L. Mapelli, contr. to (2).
13) C. Geweniger, Proc. 11th Intern. Conf. on Neutrino Phyics and Astrophysics, Dortmund 1984, K. Kleinknecht and E.A. Paschos ed.; P.G. Reutens et al., Phys. Lett. 152B, 404 (1985).
14) See also M. Greco, Proc. of the Yukon Advanced Study Institute, Whithorse (1984), N. Isgur, G. Karl and P.J. O'Donnell editors, and Frascati preprint LNF-84/61 (1984); G. Martinelli, contr. to (2).
15) For a review, see G. Altarelli, Phys. Rep. 81, 1 (1982).
16) G. Altarelli, R.K. Ellis and G. Martinelli, Nucl. Phys. B157, 461 (1979); Kubar-Andrè and F.E. Paige, Phys. Rev. D19, 221 (1979).
17) G. Parisi, Phys. Lett. 90B, 295 (1980); G. Curci and M. Greco, Phys. Lett. 92B, 175 (1980).
18) For a review, see W.J. Stirling, Proc. of the Drell-Yan Workshop, Fermilab (1982), p. 131.
19) G. Altarelli, R.K. Ellis, M. Greco and G. Martinelli, Nucl. Phys. B246, 12 (1984).
20) G. Altarelli, R.K. Ellis and G. Martinelli, Z. Phys. C27, 617 (1985).
21) C. Rubbia, contr. to (1).
22) M. Levi, contr. to (2).
23) G. Altarelli, G. Parisi and R. Petronzio, Phys. Lett. 76B, 351, (1978); H. Fritzsch and Minkowski, Phys. Lett. 74B, 384 (1978); K. Kajantie and R. Raitio, Nucl. Phys. B139, 72 (1978); F. Halzen and P.M. Scott, Phys. Rev. D18, 3378 (1978); See also, P. Aurenche and J. Lindfors, Nucl. Phys. B185, 274 (1981).
24) Yu.L. Dokshitzer, D.I. Dyakonov and S.I. Troyan, Phys. Lett. 78B, 290 (1978); Phys. Rep. 58, 269 (1980).
25) G. Parisi and R. Petronzio, Nucl. Phys. B154, 427 (1979); G. Curci, M. Greco and Y.N. Srivastava, Phys. Rev. Lett. 43, 434 (1979); Nucl. Phys. B159, 451 (1979).
26) C.Y. Lo and J.D. Sullivan, Phys. Letters 86B, 327 (1979);A. Bassetto, M. Ciafaloni and G. Marchesini, Phys. Lett. 86B, 366 (1979); S.D. Ellis and W.J. Stirling, Phys. Rev. D23, 214 (1981); H.F. Jones and J. Wyndham, Nucl. Phys. B176, 466 (1980); P.E.L. Rakow and B.R. Webber, Nucl. Phys. B187, 254 (1981); S.D. Ellis, N. Fleishorn and W.J. Stirling, Phys. Rev. D24, 1386 (1981); J.C. Collins and D.E. Soper, Nucl. Phys. B193, 381 (1981); B194, 445 (1982); B197, 446 (1982): P. Chiappetta and M. Greco, Phys. Lett. 106B, 219 (1981); Nucl. Phys. B199, 77 (1982); B221, 269 (1983); M. Pennington, Nucl. Phys. B204, 189 (1982); J. Kodaira and L. Trentadue, Phys. Lett. 112B, 66 (1982); 123B, 335 (1983).
27) H. Plothow-Besch, contr. to (2).
28) C.T.H. Davies and W.J. Stirling, Preprint CERN-TH.3853 (1984).
29) J. Kodaira and L. Trentadue, Phys. Letters 112B, 66 (1982); 123B, 335 (1983).
30) S.D. Ellis, contr. to (2).
31) W.J. Stirling, contr. to (2).
32) See for example R.F. Feynman, Photon-Hadron Interactions (Benjamin, 1972).

33) T. Akesson et al., Phys. Lett. 118B, 185 (1982); A.L.S. Angelis et al., Phys. Lett. 126B, 132 (1983).
34) UA2 Collaboration, M. Banner et al., Phys. Lett. 118B, 203 (1982); P. Bagnaia et al., Z. Phys. C20, 117 (1983).
35) UA1 Collaboration, G. Arnison et al., Phys. Lett. 123B, 115 (1983); 132B, 214 (1983).
36) E. Eichten, I. Inchliffe, K. Lane and C. Quigg, Rev. Mod. Phys. 56, 579 (1984).
37) B. Combridge, J. Kripfganz and J. Ranft, Phys. Lett. 70B, 234 (1977); R. Cutter and D. Sivers, Phys. Rev. D16, 679 (1977) and D17, 196 (1978).
38) E.J. Buckley, contr. to (2)
39) F. Pastore, contr. to (2).
40) N.G. Antoniou et al., Phys. Lett. 128B, 257 (1983).
41) R.K. Ellis, M.A. Furman, H.E. Haber and I. Inchliffe, Nucl. Phys. B173, 397 (1980).
42) D.W. Duke and J.F. Owens, Florida State Univ. Preprint, FSU/HEP/831115 (1983); see also R.K. Ellis, contr. to (1).
43) J. Kripfganz and A. Schiller, Phys. Letters 79B, 317 (1978); A. Schiller, J. Phys. G5, 1329 (1979); C.J. Maxwell, Nucl. Phys. B149, 61 (1979); T. Gottschalk and D. Sivers, Phys. Rev. D21, 102 (1980); Z. Kunszt and E. Pietarien, Nucl. Phys. B164, 45 (1980).
44) F.A. Berends et al., Phys. Lett. 103B, 124 (1981).
45) Z. Kunszt and d and E. Pietarinen, Phys. Lett. 132B, 453 (1983).
46) M. Greco, Z. Phys. C26, 567 (1985).
47) UA2 Collaboration, P. Bagnaia et al., Phys. Lett. 144B, 283 (1984).
48) P. Ghez, contr. to (2).
49) UA2 Collaboration, P. Bagnaia et al., Phys. Lett. 144B, 291 (1984).
50) See also G. Marchesini and B.R. Webber, Nucl. Phys. B238, 1 (1984) and B.R. Webber, Nucl. Phys. B238, 492 (1984).
51) H.M. Georgi, S.L. Glashow, M.E. Machacek and D.V. Nanopoulos, Phys. Rev. Lett. 40, 692 (1978).
52) K.J.F. Gaemers and F. Hoogeveen, Phys. Lett. 146B, 347 (1984).
53) M. Greco, Phys. Lett. 156B, 109 (1985).